A computational fluid Dynamics (CFD) model intended for fluid flow prediction inside a modified atmospheric packaging container

THE SCHOOL OF PACKAGING

2010 Inverse Problems Symposium

MICHIGAN STATE UNIVERSITY

Brajesh Tripathi, Maria Rubino & Rafael Auras

School of Packaging, Michigan State University, East Lansing, MI

Introduction and Objectives

Modified atmospheric packaging (MAP) is one of the techniques used to maintain the safety and freshness of product inside a package where the atmosphere inside the package is modified and further maintained during the life of the product. The initial distribution of gases inside a package plays an important role for determining the product shelf life. A food container used for packaging food products in a MAP machine was simulated in the present work with objectives of;

- Visualisation of diffusion through the inlet.
- Variation of gas dynamics throughout the container.

Methodology

Schematic of computational geometry is shown in Fig.1. The size of inlet and outlet are 0.5cm and 0.8cm, respectively and denoted by incoming and outgoing arrows. The geometry of the empty food container is divided in variable hexahedral meshes to predict the fluid flow behavior. The cases of inlet air direction and variation in flow rate were analyzed inside the atmospheric enhancement with the proper circulation of a disinfecting CO_2 gas.

- The flow field inside the container was generated by directly solving the Navier-Stokes equations over the finite volume method for an incompressible Newtonian fluid with constant viscosity.
- The governing equations for conservation of mass, Eq.1 and momentum, Eq.2 using mean and fluctuating values $u_i = \bar{u}_i + u_i'$ for components are;

$$\frac{\partial \rho}{\partial t} + \frac{\partial \rho}{\partial x_i}(\rho u_i) = 0 \ldots (1), \quad \frac{\partial}{\partial x_i}(\rho u_i u_j) = -\frac{\partial \rho}{\partial x_i}\left[\mu\left(\frac{\partial u_i}{\partial x_j} + \frac{\partial u_j}{\partial x_i} - \frac{2}{3}\partial_{ij}\frac{\partial u_i}{\partial x_j}\right)\right] + \frac{\partial}{\partial x_j}(-\rho \overline{u_i' u_j'}) \ldots (2)$$

- RNG k-ε model: The equations for kinetic energy (k), Eq. 3 and dissipation of kinetic energy (ε), Eq. 4 are;

$$\frac{\partial}{\partial x_j}(\rho k u_j) = \frac{\partial}{\partial x_j}\left[\left(\mu + \frac{\mu_t}{\sigma_k}\right)\frac{\partial k}{\partial x_j}\right] + G_k - \rho\varepsilon \ldots (3), \quad \frac{\partial}{\partial x_j}(\rho \varepsilon u_j) = \frac{\partial}{\partial x_j}\left[\left(\mu + \frac{\mu_t}{\sigma_\varepsilon}\right)\frac{\partial \varepsilon}{\partial x_j}\right] - \rho C_2 \frac{\varepsilon^2}{k + \sqrt{\varepsilon \nu}} \ldots (4)$$

- where model constants are $G_k = \mu_t S^2$, C_2=1.9, σ_k=1.0, σ_ε=1.2.
- A reverse flow field was generated at the outlet, and it was concerned with iteration correction, error criteria and relaxation factors. A separate flow field was generated by initializing the solution at outlet for inverse CFD simulation with no slip boundary condition.

Schematic

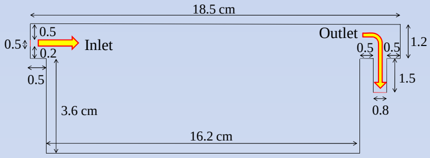

Fig. 1: Schematic of Computational Geometry

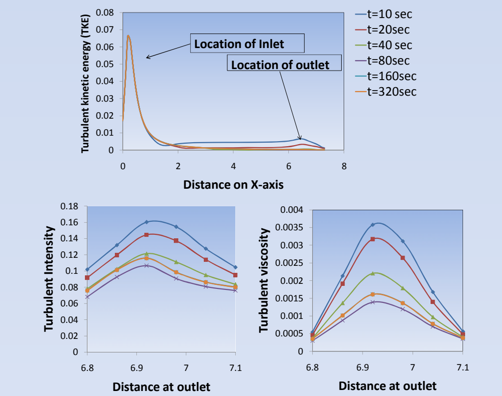

Fig. 2. TKE, Turbulent Intensity, Turbulent Viscosity plots at t=60sec

Contours of Inverse Simulation at Re=454

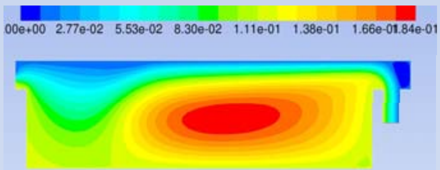

Fig. 3: Stream Function contours

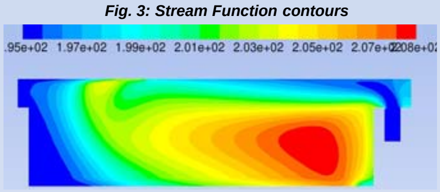

Fig. 4: Static Temperature plots

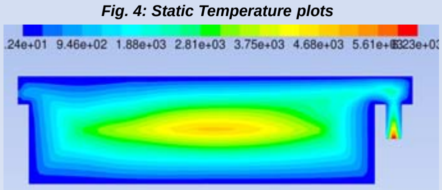

Fig. 5: Contours of Turbulent Reynolds number

Sensitivity analysis

Sensitivity derivative was calculated by Complex Variable Formulation and approximation to output error, Eq.5 is;

$$\delta u_i = \left[\sum_{j=1}^{n} S_{ij}^2 \delta k_j\right]^{1/2} \ldots (5)$$

Table 1: Comparison of direct and inverse simulation at Re=454

Time Step size	Iteration		CPU* time in seconds		Converge (Power of 10)	
>>	Direct	Inv.	Direct	Inv.	Direct	Inv.
10	473	456	41	15.1	-04	-05
20	729	681	29	25.3	-04	-06
40	1225	1060	46	53.4	-05	-07
80	1679	1460	77	65.2	-05	-08
160	2551	2260	163	151.8	-05	-08
320	4119	3860	435	354.6	-07	-08

*128 nodes, duel core, 2.2 GHz, 8GB RAM, 1GB Ethernet

Expected Results

- CFD predictions of the inverse formulation advances quickly towards the converged solution for the MAP food packaging container.
- Flow fields were also obtained for variations of flow rate and direction angle. Formation of small vortices near the outlet was observed in the inverse flow field.
- The calculation period of converged solution was always lower for inverse flow conditions.

Acknowledgement: Authors are thankful to USDA (grant no. 2008-01573) under "National Integrated Food Safety Initiative" for financial support and HPCC, MSU for computational facility.